11-15-2022

Relationship of neurite architecture to brain activity during task-based fMRI

Christin Schifani

Colin Hawco

Arash Nazeri

Aristotle N Voineskos
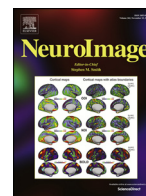
Relationship of neurite architecture to brain activity during task-based fMRI

Christin Schifani [a], Colin Hawco [a,b,d], Arash Nazeri [c], Aristotle N. Voineskos [a,b,d,*]

[a] *Kimel Family Translational Imaging-Genetics Research Laboratory, The Centre for Addiction and Mental Health, Toronto, ON, Canada*
[b] *Department of Psychiatry, University of Toronto, Toronto, ON, Canada*
[c] *Mallinckrodt Institute of Radiology, Washington University School of Medicine, St. Louis, MO, United States*
[d] *Institute of Medical Science, University of Toronto, Toronto, ON, Canada*

A B S T R A C T

Functional MRI (fMRI) has been widely used to examine changes in neuronal activity during cognitive tasks. Commonly used measures of gray matter macrostructure (e.g., cortical thickness, surface area, volume) do not consistently appear to serve as structural correlates of brain function. In contrast, gray matter microstructure, measured using neurite orientation dispersion and density imaging (NODDI), enables the estimation of indices of neurite density (neurite density index; NDI) and organization (orientation dispersion index; ODI) in gray matter. Our study explored the relationship among neurite architecture, BOLD (blood-oxygen-level-dependent) fMRI, and cognition, using a large sample ($n = 750$) of young adults of the human connectome project (HCP) and two tasks that index more cortical (working memory) and more subcortical (emotion processing) targeting of brain functions. Using NODDI, fMRI, structural MRI and task performance data, hierarchical regression analyses revealed that higher working memory- and emotion processing-evoked BOLD activity was related to lower ODI in the right DLPFC, and lower ODI and NDI values in the right and left amygdala, respectively. Common measures of brain macrostructure (i.e., DLPFC thickness/surface area and amygdala volume) did not explain any additional variance (beyond neurite architecture) in BOLD activity. A moderating effect of neurite architecture on the relationship between emotion processing task-evoked BOLD response and performance was observed. Our findings provide evidence that neuro-/social-affective cognition-related BOLD activity is partially driven by the local neurite organization and density with direct impact on emotion processing. In vivo gray matter microstructure represents a new target of investigation providing strong potential for clinical translation.

1. Introduction

Functional MRI (fMRI) examines brain activity by measuring the blood-oxygen-level-dependent (BOLD) signal, which is driven by an oversupply of local blood flow following increased neural activity. Although fMRI has been widely used to examine changes in brain activity during cognitive tasks, there is still debate about which specific aspects of neural processing drive the BOLD response (Drew, 2019; Ekstrom, 2010; Hall et al., 2016). Neural signals within and between brain regions are propagated via neurites, comprising axons transmitting signals between regions and dendrites receiving neural information from synapses and propagating them (Jessell and Kandel, 1993). Neurite organization can influence the neural dynamics in terms of how efficiently information is transmitted; for example, dendritic complexity contributes to the quantity of inputs captured from other neurons

(Lefebvre et al., 2015). Although the function and organizing of neurites is a key feature of local neuronal processing, which is the presumed neurophysiological basis for the BOLD signal, the relationship between gray matter neurite microstructure and BOLD activity remains largely unexplored in humans.

Measures of gray matter macrostructure (i.e., cortical thickness and surface area or volume) have been linked to performance in a variety of cognitive tasks targeting neurocognitive and social cognitive processes (reviewed by Karantonis et al., 2021; Kaup et al., 2011; Khalil et al., 2022; Salthouse, 2011). However, the literature is conflicting in terms of relating gray matter macrostructure to BOLD response and cognition. While some studies have related higher-order cognitive function such as working memory separately to cortical thickness and BOLD response in the prefrontal cortex (PFC) (Ehrlich et al., 2012; Yuan and Raz, 2014), others have shown no association between working memory-evoked

BOLD activity in PFC and both cortical thickness (Owens et al., 2018; Zacharopoulos et al., 2020) and surface area (Evangelista et al., 2021). For contrary results see (Zacharopoulos et al., 2020) reporting a negative association between left frontal pole surface area and BOLD response towards working memory. This lack of relationships may not be surprising given that gray matter macrostructure is composed of various microstructural elements including the neuropil (neuronal bodies, dendrites and synapses), glial cells, axons, and vasculature (Zatorre et al., 2012) limiting its specificity and interpretability related to neurite characteristics. For lower-level social cognitive function, such as emotional processing, where the amygdala is a key region, relationships with macrostructure (i.e., volume) (Pera-Guardiola et al., 2016; Zhao et al., 2013) and function (Derntl et al., 2009; Habel et al., 2007) have been reported separately.

Advances in multishell diffusion-weighted MRI (dMRI) acquisition and modeling, such as neurite orientation dispersion and density imaging (NODDI) (Zhang et al., 2012), have made it possible to model distinct aspects of gray matter microstructure related to neurites (Mah et al., 2017). Using compartmentalization of brain tissue enables the estimation of indices of neurite density (NDI; how many axons/dendrites are in a given space) and orientation dispersion (ODI; the complexity/branching/organization of dendritic trees) (Nazeri et al., 2020). Recent work shows a clear distinction in patterns of NDI and ODI distribution across the cortical gray matter (Fukutomi et al., 2018). While NDI seemed to correspond well with the distribution of myelin (myeloarchitecture) (Braak, 1980; Nieuwenhuys, 2013), ODI was interpreted as reflecting regional variations in the cortical cytoarchitecture (Von Economo, 2009; von Economo and Koskinas, 1925). These indices of neurite architecture may be related to working memory and emotion recognition performance (Nazeri et al., 2015, 2017; Yasuno et al., 2020), functional connectivity (Morris et al., 2016; Nazeri et al., 2015) and BOLD response towards basic stimuli (i.e., motor activity, visual stimuli and reading) (Teillac et al., 2017).

Using NODDI-based measures of gray matter microstructure, we studied the relationship among neurite architecture, BOLD fMRI, and cognition, using the human connectome project (HCP) dataset (S900 release). The HCP acquisitions included fMRI in several tasks targeting different cognitive domains from more basic, lower-order social cognition (emotional processing) up to complex, higher-order neurocognition (working memory) (Barch et al., 2013). For this initial study of the relationship between neurite architecture, BOLD fMRI, and cognition, we constrained our analyses by choosing two of the most commonly used tasks in the literature with a very clear, repeatedly shown and reliable activation pattern (Plichta et al., 2012; Sabatinelli et al., 2011; Sergerie et al., 2008), covering domains of working memory and emotion processing, as we have done in former studies of our group (Ameis et al., 2011; Barr et al., 2013; Hawco et al., 2020; Jacobs et al., 2021; Nazeri et al., 2017; Oliver et al., 2019, 2021; Voineskos et al., 2021). These two tasks index different cognitive domains/constructs, different brain networks, and represent relatively higher-order and lower-order cognitive tasks. We hypothesized that the BOLD response in key regions, specifically dorsolateral prefrontal cortex (DLPFC) for working memory (Barbey et al., 2013) and amygdala for emotional processing (López et al., 1999; Vuilleumier et al., 2001), would be associated with neurite density and/or orientation dispersion, estimated using the NODDI model, independent of macrostructural measures (i.e., cortical thickness and surface area or subcortical volume). We further hypothesized that the underlying neurite architecture would impact the BOLD response-task performance relationship in those key regions.

2. Methods

2.1. Participants

Structural, multishell dMRI and task fMRI data from young, healthy adults were obtained from the WU-Minn Human Connectome Project (Barch et al., 2013; Glasser et al., 2016b; Van Essen et al., 2013), downloaded from ConnectomeDB as part of the S900 release (http://db.humanconnectome.org). Of 900 participants, only those who completed both working memory and emotion processing fMRI tasks, the multishell dMRI scan and had good quality data for all modalities (including structural scans) were included (see "Quality control" section below), leaving a sample of $n = 750$ (see Supplementary Table 1 for sample characteristics). This study received approval from the local ethics board and data were accessed with permission of HCP.

2.2. Acquisition and processing of downloaded data

All subjects were scanned using the same imaging protocol on modified Siemens Skyra scanners. For multishell dMRI the following parameters were used, as described before (Van Essen et al., 2013): TR = 5520 ms, TE = 89.5 ms, gradient duration (δ) = 10.6 ms, gradient separation (Δ) = 43.1 ms, image resolution = 1.25×1.25×1.25 mm^3, phase partial Fourier = 0.75, and multiband factor = 3. The dMRI data were acquired with 3 b-values of nominally 1000, 2000 and 3000 s/mm^2 with 90 gradient directions at each shell. Additionally, 18 $b = 0$ images were collected. For each scan, the dMRI data were acquired twice with opposite phase encoding directions to correct for susceptibility-induced image distortions. During the preprocessing, images with opposite phase encoding directions were combined to obtain the final image. As downloaded, the data were preprocessed with corrections for gradient nonlinearity distortions, susceptibility-induced distortions, head motion, and eddy current artifacts (Glasser et al., 2013; Sotiropoulos et al., 2013).

The fMRI task activation maps from specific first-level contrasts across two cognitive paradigms were used (selected contrast in parentheses): N-back working memory (2-back minus 0-back) and emotion processing (faces minus shapes). The HCP n-back working memory task consisted of 0-back and 2-back trials containing images of faces, places, tools and body parts. We used the working memory load contrast (2-back minus 0-back) across all the available image categories as described before (Barch et al., 2013). The HCP emotion processing task consisted of trials with negative faces (sad or angry) or shapes (ovals in different orientations) (Hariri et al., 2002). The only available contrast consisted of faces minus shapes which was used in the current study, as previously described (Barch et al., 2013). The acquisition parameters for the task fMRI scans were the following: Whole-brain EPI images were acquired with a 32-channel head coil with TR = 720 ms, TE = 33.1 ms, flip angle = 52°, BW = 2290 Hz/Px, in-plane FOV = 208×180 mm, 72 slices, 2.0 mm isotropic voxels, with a multi-band acceleration factor of 8 (Feinberg et al., 2010). For each task, the HCP collected two runs which differed with respect to the MRI phase encoding direction (left to right or right to left). The HCP fMRI tasks are described in detail elsewhere (Barch et al., 2013). Data to download were selected from the surface smoothed 8 mm FWHM using the HCP minimal preprocessing pipeline (Glasser et al., 2013). This pipeline included motion correction, distortion correction, registration to standard space, and generation of a grayordinate (cortical surface) time-series for each task run (Fig. 1). Statistical analyses were performed in FSL (www.fmrib.ox.ac.uk/fsl). Fixed-effects ("first-level") analysis was performed on each run separately, including the smoothing stage (performed on the cortical surface), and then the two runs for each task were combined via a second fixed-effects analysis. For each participant, the HCP provided t-maps for each task which were downloaded and used. We used t-maps as opposed to Beta estimates as the t-values are deweighted in noisy voxels due to the higher variance. Individual fMRI-task-performance data, comprising the performance of 2-back (n-back task) and emotional faces (emotion processing task) trials, were also downloaded.

2.3. NODDI calculation

The biophysical NODDI model allows to estimate neurite architecture using three compartments: (1) intracellular (restricted diffusion;
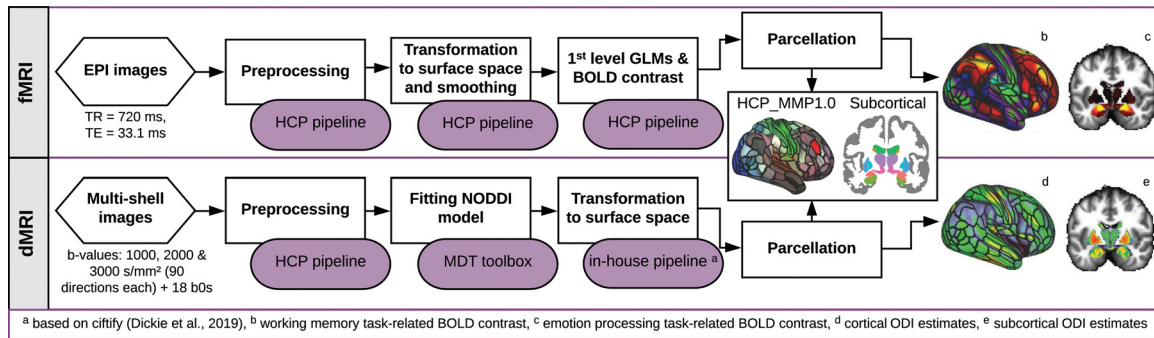
Fig. 1. Schematic diagram showing the processing steps for the functional MRI (fMRI) and diffusion-weighted MRI (dMRI) scan data.

bounded by the membrane of neurites and myelin sheaths), (2) extracellular (anisotropic, hindered diffusion; outside of neurites and potentially including glial cells), and (3) CSF compartments (isotropic diffusion). These three microstructural compartments can provide independent measures of: (i) neurite density by estimating the fraction of water restricted in the intracellular compartment (neurite density index [NDI]) which relates to the amount of neurites and (ii) neurite organization/spatial configuration by estimating dispersion (orientation dispersion index [ODI]). CSF compartment estimates in each voxel ensure that each index is fully adjusted for CSF contamination (Zhang et al., 2012).

Using the downloaded, preprocessed dMRI data, the NODDI model was fitted using the MDT toolbox v.0.20 (Harms et al., 2017) (www.mdt-toolbox.readthedocs.io) batchfit algorithm (Fig. 1). Validated on an internal sample of data, NODDI fitting using the MDT toolbox gave the same results as with the original NODDI matlab toolbox (http://mig.cs.ucl.ac.uk/) (data not shown). The MDT output included NDI and ODI maps in subject space.

2.4. Surface reconstruction of NODDI data

Individuals' preprocessed structural images (0.7 mm isotropic T1-weighted [T1w]) and their 32k space projections were downloaded from HCP and used for surface mapping of the NODDI maps. In brief, the structural images were preprocessed (corrected for gradient nonlinearity, readout, and bias field; aligned to AC-PC "native" space; then registered to MNI 152 space using FSL's FNIRT). The native space images were used to generate individual white and pial surfaces (Glasser et al., 2013) using the FreeSurfer (https://surfer.nmr.mgh.harvard.edu/) and HCP pipelines (https://github.com/Washington-University/Pipelines). In the post-FreeSurfer pipeline, the individual subject's native-mesh surfaces were registered using a multimodal surface matching (MSM) algorithm (Robinson et al., 2014) with MSMSulc to the Conte69 folding-based template (Van Essen et al., 2012).

Individual dMRI data were registered to each individual's structural T1w AC-PC space using the b0 volume and the white surface with the BBR cost function in FSL v.6.0.0 (Greve and Fischl, 2009). The diffusion gradient vectors were rotated based on the rotational information of the b0 to T1w transformation matrix. A combined transform (b0 to T1w and T1w to MNI) was used to warp the NODDI maps (NDI and ODI) into MNI space. The NODDI maps were mapped onto the cortical surface using an algorithm weighted towards the cortical mid-thickness (Glasser and Van Essen, 2011) and Connectome Workbench v.1.3.2 (https://github.com/Washington-University/workbench). For each mid-thickness surface vertex on the native mesh, the algorithm identified cortical ribbon voxels within a cylinder orthogonal to the local surface. The surface maps were subsequently resampled based on MSMAll surface registration (Glasser et al., 2016a; Robinson et al., 2014) and onto the 32k group average surface mesh (Dickie et al., 2019).

2.5. Quality control

HCP's openly available issue websites (https://wiki. humanconnectome.org/display/PublicData/HCP+Data+Release+ Updates%3A+Known+Issues+and+Planned+fixes and https://wiki. humanconnectome.org/pages/viewpage.action?pageId=88901591) and visual checks were used to exclude data of poor quality, with major processing issues and non-usable task data.

2.6. Parcellation and region of interest (ROI) selection

The relationship between gray matter neurite architecture and task-related BOLD activity was explored using an ROI approach. Given its role and strong activation in working memory (Fig. 2) (Barbey et al., 2013), the DLPFC was chosen a priori for the n-back task-related BOLD activity associations with neurite architecture. Specifically, region p9–46v from the HCP Multi-modal Cortical Parcellation 1.0 (HCP_MMP1.0 210P MPM version) (Glasser et al., 2016a) was selected, as this region showed the strongest activity in the group statistical map of the fMRI n-back task (Fig. 2). For the emotion processing task, the amygdala was selected due to its role in emotion processing and strong activation to emotional tasks, especially involving faces with negative emotions such as fear and anger (Fig. 4A) (Sabatinelli et al., 2011; Vuilleumier et al., 2001). *Microstructure and BOLD:* Each individual's mean values for NDI, ODI and task t-statistic were extracted separately for both the left and right hemispheres from the selected regions (for a total of 4 ROIs; Connectome Workbench v.1.3.2). For the subcortical gray matter ROIs (left and right amygdala), outer ROI voxels (layer of one voxel) with NDI values ≥ 0.75 were identified and removed from NDI and ODI maps to avoid partial volume effects and potential residual white matter. *Macrostructure:* Cortical thickness and surface area of the pial surface were extracted separately for both the left and right DLPFC (Connectome Workbench v.1.3.2). Subcortical volume values of the amygdala (left and right; in mm^3) were provided by HCP as part of the FreeSurfer outputs and were corrected for intracranial volume.

2.7. Statistical analysis

All analysis was performed using R (v.4.0.2). The lm.beta package (v.1.5–1; https://cran.r-project.org/web/packages/lm.beta/index. html) was used for standardization of beta values. The ggplot2 package (v.3.3.2; https://cran.r-project.org/web/packages/ggplot2/index. html) and Connectome Workbench (v.1.3.2; https://www. humanconnectome.org/software/connectome-workbench) were used for visualization. Interaction plots and simple slope analysis were generated with the interactions package (v.1.1.5; https://cran.r-project.org/web/packages/interactions/index.html) using the interact_plot and sim_slope functions, respectively.

Hierarchical regressions were used to study the relationships between neurite architecture (i.e. NODDI indices) and BOLD activity.
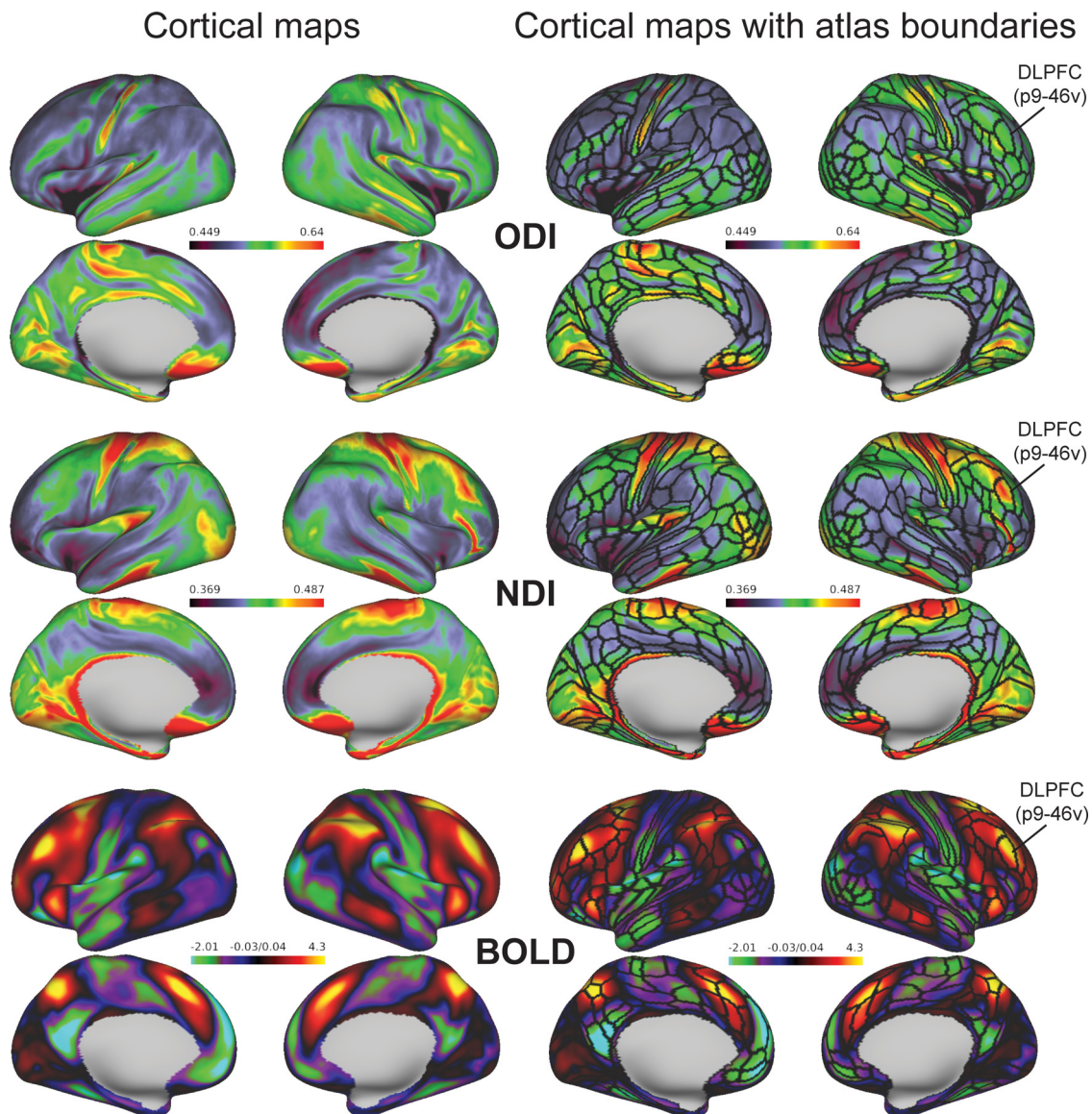
Fig. 2. Cortical NODDI indices (NDI and ODI) and n-back task-related BOLD activity (2-back minus 0-back) maps. Group average values for ODI (top), NDI (middle) and BOLD (group t-statistic, bottom) in cortical regions including the DLPFC (shown in surface space), (left) without any overlay and (right) overlaid by the HCP Multi-modal Cortical Parcellation 1.0.

Macrostructural measures were incorporated in order to examine specificity of the neurite architecture-BOLD activity relationship. For example, any relationships between ODI or NDI and BOLD activity could represent general structural changes (i.e., changes in macrostructure), as opposed to changes specific to microstructure. For the DLPFC, cortical thickness and surface area in the DLPFC ROIs were used as macrostructural measures, while in the amygdala ROIs, amygdala volume (corrected for intracranial volume) was used. Separately for each of the four ROIs (left DLPFC, right DLPFC, left amygdala, and right amygdala), a three-step hierarchical regression was performed with BOLD activity as the dependent variable. Age and sex were entered at step one of the regression to control for demographic differences (ongoing alterations in NDI and ODI from late adolescence to adulthood have been reported as well as sex differences (Tsuchida et al., 2021)). Neurite architectural variables (ODI and NDI) were entered at step two, and the macrostructural measure (DLPFC thickness and surface area or amygdala volume) at step three. The relationship variables were entered in this order as it seemed plausible given that neurite architectural measures (ODI and NDI) are underlying at least partially the measures of gross brain structure such as cortical thickness (Fukutomi et al., 2018; Genç et al., 2018),

surface area and subcortical volume. Step two regression models were followed by partial correlation analysis (regressing out age and sex) of the relationship between the separate NODDI indices, ODI and NDI, and BOLD activity.

Neurite architecture was also examined as a moderator of the relationship between BOLD activity and task performance. We first established the relationship between BOLD activity and task performance using linear regressions per ROI (corrected for age and sex). This was followed by the moderation analyses, performed separately for each of the four ROIs (left DLPFC, right DLPFC, left amygdala, and right amygdala). For the DLPFC and amygdala ROIs respectively, performance of the 2-back or emotional faces tasks were used as the dependent variables. Either ODI or NDI was entered in the first step of the regression analysis together with BOLD activity, age and sex. In the second step, the interaction between BOLD and either ODI or NDI was added, to examine the moderating effect of neurite organization or density on the relationship between BOLD activity and task performance; a significant change in R^2 would represent a moderation between BOLD activity, neurite architecture, and task performance. Where residuals of the moderation analysis regressions were not normally distributed, we explored permu-
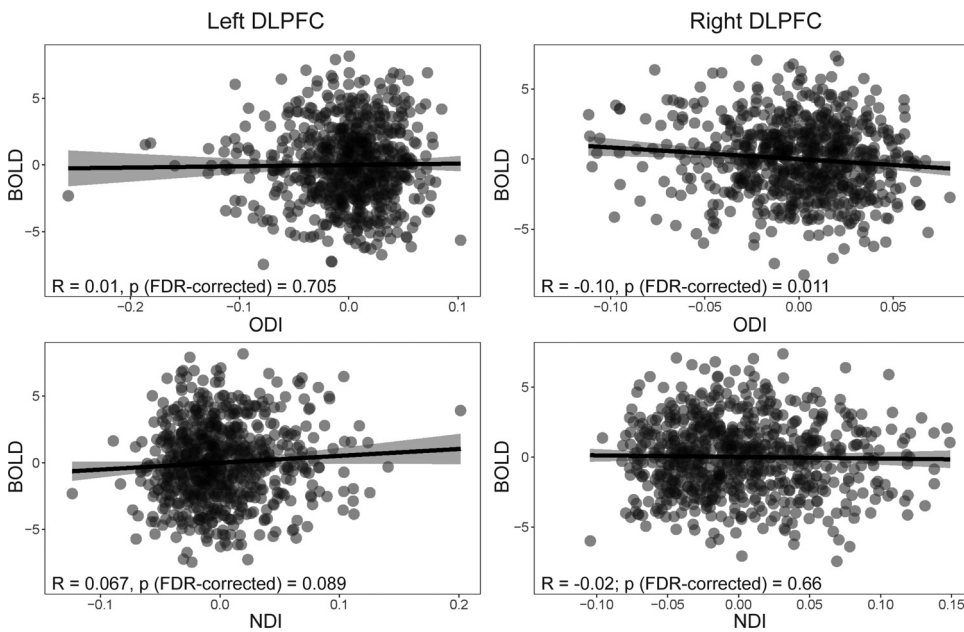
Left DLPFC
Right DLPFC

Fig. 3. Associations between n-back task-related BOLD activation and NODDI indices in DLPFC. Partial correlations of ODI (top row) and NDI (bottom row) with BOLD activity, corrected for age and sex. Association of ODI in right DLPFC was significant after multiple comparisons' correction using FDR.

tation testing with the lmPerm package for R (v.2.1.0; https://cran.r-project.org/web/packages/lmPerm/index.html) using the lmp function with 'Prob' permutation option. Affected models are described in the results section.

P-values of subsets of analyses were corrected for multiple comparisons (4 ROIs [left DLPFC, right DLPFC, left amygdala, right amygdala] within each step of each model run, i.e., hierarchical regression and moderation analyses; FDR correction) as indicated in the results. In this context, p-values of ≤ 0.05 were considered statistically significant.

Code is made available via github (https://github.com/cschifani/HCP_NODDIvsfMRI).

3. Results

3.1. Relationships of task-related BOLD activation with neurite architecture (ODI and NDI) and macrostructure (cortical thickness, surface area and subcortical volume)

3.1.1. Neurite architecture but not cortical thickness or surface area explained variability in n-back task-related BOLD activation in DLPFC

Whole-brain group averages for NDI and ODI, and 2nd-level group n-back BOLD activity are shown in Fig. 2.

Hierarchical regression analysis for right DLPFC revealed that introducing the microstructural variables (ODI and NDI; step two), after controlling for age and sex (step one), explained additional variance in BOLD activity ($F_{2,745} = 4.05$, $p = 0.018$), with an increase in R^2 of 0.01. However, in step three, adding right DLPFC thickness and surface area (macrostructural variables) was not significant ($F_{2,743} = 2.44$, $p = 0.088$). When either four or all six independent variables were included in steps two or three of the regression model, respectively, ODI was the only significant predictor of BOLD activity in right DLPFC (step 2: beta = -0.10, $t = -2.79$, p (FDR-corrected) = 0.011; step 3: beta = -0.11, $t = -2.98$, p (FDR-corrected) = 0.012) which uniquely explained 1% of the total variance in BOLD activity (for further details see Supplementary Table 2, right). This was further confirmed by partial correlation analysis (Fig. 3, right), showing a significant negative association of BOLD activity in right DLPFC with ODI ($R = -0.10$, p (FDR-corrected) = 0.011) but not with NDI ($R = -0.02$; p (FDR-corrected) = 0.66).

For left DLPFC, after controlling for age and sex, introducing the microstructural variables (ODI and NDI, step two) and macrostructural variables (cortical thickness and surface area, step three) did not explain

additional variance in BOLD activity (model two: $F_{2,745} = 1.72$, $p = 0.18$; model three: $F_{2,743} = 2.25$, $p = 0.11$) (for further details see Supplementary Table 2, left). This was further confirmed by partial correlation analysis (Fig. 3, left), showing no significant association of BOLD activity in left DLPFC with either ODI ($R = 0.01$, p (FDR-corrected) = 0.71) or NDI ($R = 0.067$, p (FDR-corrected) = 0.089).

Exploratory relationships between neurite architecture and BOLD activity in other cortical brain regions can be found in Supplementary Figure 1.

3.1.2. Neurite architecture but not subcortical volume explained variability in emotion processing task-related BOLD activation in amygdala

Subcortical group averages for NDI and ODI, and 2nd-level group emotional processing task BOLD activity are shown in Fig. 4A.

Hierarchical regression analysis for right amygdala revealed that introducing the microstructural variables (ODI and NDI; step two), after controlling for age and sex (step one), explained additional variance in BOLD activity ($F_{2,745} = 11.20$, $p = 1.61 \times 10^{-5}$), with a change in R^2 of 0.03. However, adding right amygdala volume to the regression (step three) did not explain significant additional variance ($F_{1,744} = 3.22$, $p = 0.073$). In both steps two or three of the regression model both ODI (step 2: beta = -0.11, $t = -2.90$, p (FDR-corrected) = 0.015; step 3: beta = -0.12, $t = -3.09$, p (FDR-corrected) = 0.0095) and NDI (step 2: beta = -0.13, $t = -3.33$, p (FDR-corrected) = 0.0037; step 3: beta = -0.14, $t = -3.44$, p (FDR-corrected) = 0.0041) were significant predictors of BOLD activity in right amygdala which uniquely explained similar amounts of variance (each about 1.5%) (for further details see Supplementary Table 3, right). This was further confirmed by partial correlation analysis (Fig. 4B, right), which showed significant negative associations of BOLD activity in right amygdala with ODI ($R = -0.12$, p (FDR-corrected) = 0.0036) and NDI ($R = -0.13$; p (FDR-corrected) = 0.0018).

The hierarchical regression analysis for left amygdala revealed that introducing the microstructural variables (ODI and NDI; step two), after controlling for age and sex (step one), explained additional variance in BOLD activity ($F_{2,745} = 6.10$, $p = 0.0024$), with a change in R^2 of 0.02. However, adding left amygdala volume to the regression (step three), did not explain additional variance ($F_{1,744} = 0.009$, $p = 0.92$). In both steps two or three of the regression model, NDI was a significant predictor of BOLD activity in left amygdala (step 2: beta = -0.11, $t = -2.81$, p (FDR-corrected) = 0.010; step 3: beta = -0.11, $t = -2.81$, p (FDR-corrected) = 0.012), while ODI was not statistically significant (step 2:
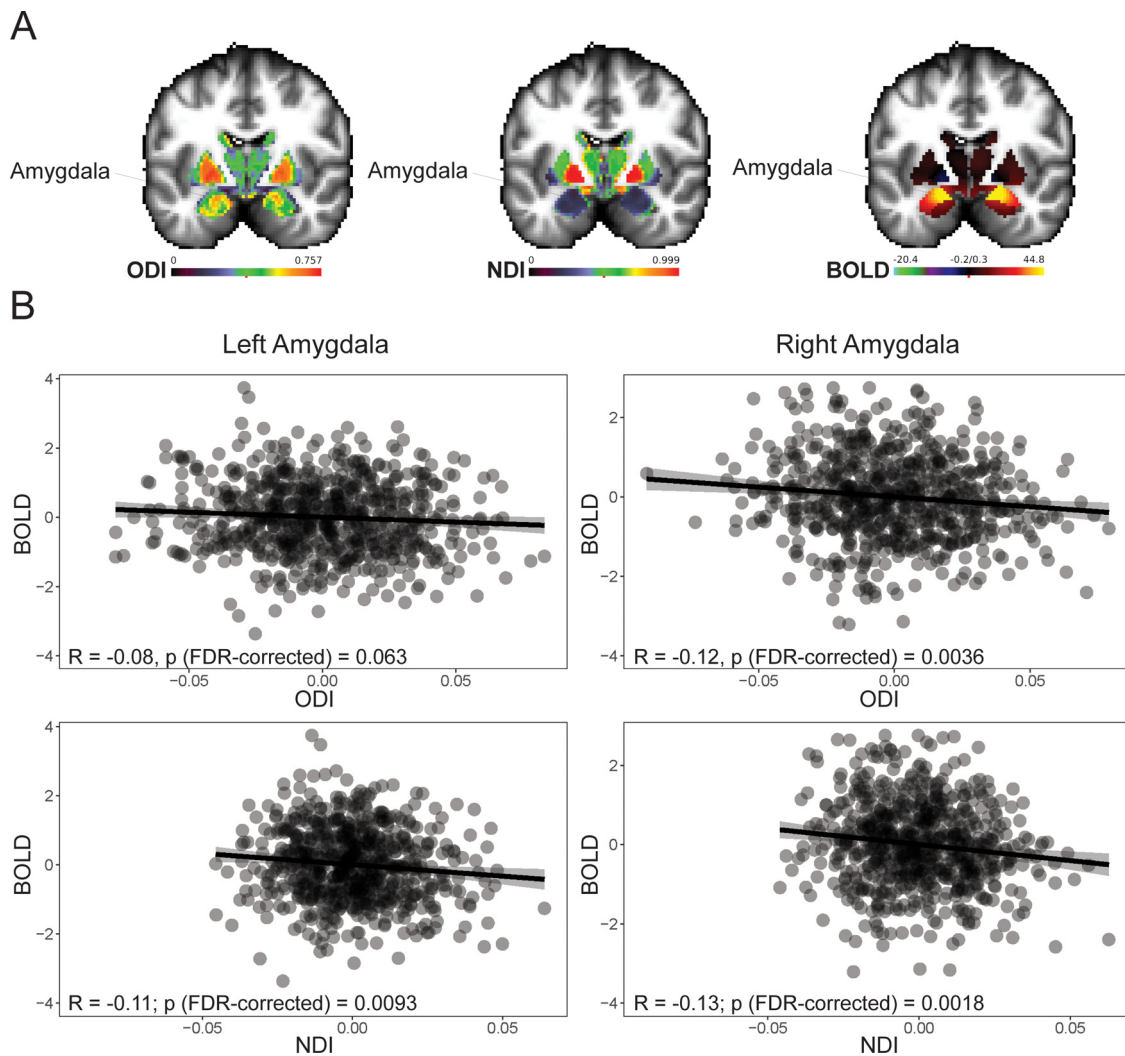
Fig. 4. Associations between BOLD activity (faces minus shapes) and NODDI indices in amygdala. (A) Group average values for ODI (left), NDI (middle) and BOLD (group t-statistic, right) in subcortical regions including the amygdala. (B) Partial correlations of ODI (top row) and NDI (bottom row) with BOLD activity, corrected for age and sex. Associations of ODI in right amygdala, and NDI in right and left amygdala, were significant after multiple comparisons' correction using FDR.

beta $= -0.07$, $t = -1.90$, p (FDR-corrected) $= 0.078$; step 3: beta $= -0.07$, $t = -1.90$, p (FDR-corrected) $= 0.066$). ODI and NDI uniquely explained about 0.6 and 1% of the variance in BOLD activity in left amygdala, respectively (for further details see Supplementary Table 3, left). This was further confirmed by partial correlation analysis (Fig. 4B, left), showing a significant negative association of BOLD activity in left amygdala with NDI ($R = -0.11$; p (FDR-corrected) $= 0.0093$) while the association with ODI did not survive multiple comparisons' correction ($R = -0.08$, p (FDR-corrected) $= 0.063$).

These results generally confirmed significant relationships between higher ODI or NDI indices and lower BOLD activity during emotion processing (Fig. 4B) and this relationship did not seem to be explained by macrostructure (amygdala volume).

3.2. Impact of neurite architecture on the relationship between task-related BOLD activation and task performance

3.2.1. No moderating effect of neurite architecture on the relationship between n-back task-related BOLD activation in DLPFC and working memory task performance

As expected, both left and right DLPFC BOLD activity were associated with 2-back task performance (left DLPFC: beta $= 0.36$, df $= 746$, $t = 10.84$, p (FDR-corrected) $= 8 \times 10^{-16}$; right DLPFC beta $= 0.35$,

df $= 746$, $t = 10.28$, p (FDR-corrected) $= 4 \times 10^{-16}$; corrected for age and sex).

To study the moderating effect of neurite architecture on this relationship, BOLD activity and NODDI indices (ODI or NDI) for left or right DLPFC were entered into the first step of the regression analysis (together with age and sex). In the second step of the regression analysis, the interaction term between the NODDI indices and BOLD activity was entered, and it did not result in any significant change in variance explained in 2-back task performance (ODI: left DLPFC: $\Delta R^2 = 0.0001$, $F_{1, 744} = 0.14$, p (FDR-corrected) $= 0.95$; right DLPFC: $\Delta R^2 = 0$, $F_{1, 744} = 0.06$, p (FDR-corrected) $= 0.80$; NDI: left DLPFC: $\Delta R^2 = 0.0002$, $F_{1, 744} = 0.18$, p (FDR-corrected) $= 0.67$; right DLPFC: $\Delta R^2 = 0.0004$, $F_{1, 744} = 0.40$, p (FDR-corrected) $= 0.70$).

3.2.2. Moderating effect of neurite architecture on the relationship between emotion processing task-related BOLD activation in amygdala and emotion processing performance

As expected, both left and right amygdala BOLD activity were associated with faces task performance (left amygdala: beta $= 0.13$, df $= 746$, $t = 3.54$, p (FDR-corrected) $= 0.00056$; right amygdala: beta $= 0.08$, df $= 746$, $t = 2.19$, p (FDR-corrected) $= 0.029$; corrected for age and sex). Given a non-normal distribution of the models' residuals, sensitivity analysis was conducted where p-values were calculated using per-
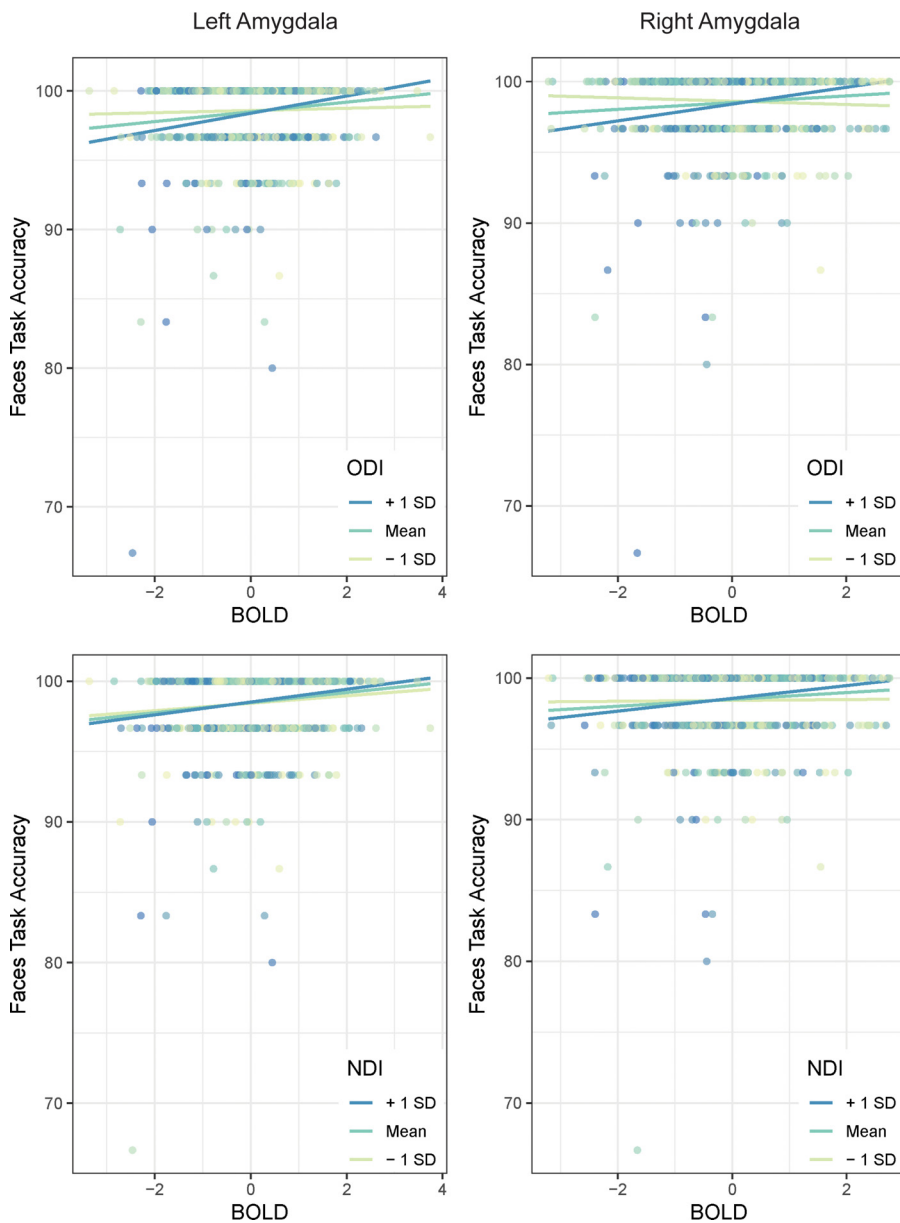
Left Amygdala

Right Amygdala

Fig. 5. Neurite architecture as a moderator of the relationship between emotion processing task-related BOLD activation and task performance. Simple slopes of the associations between BOLD activity and faces task performance for 1 SD below the average of the NODDI indices (light green), the average of the NODDI indices (green-blue) and 1 SD above the average of the NODDI indices (dark blue) for (left) left and (right) right amygdala. ODI is depicted in upper row; NDI in lower row. BOLD, ODI and NDI are corrected for age and sex.

mutation tests. The direction of results stayed the same (FDR-corrected p-values; left amygdala: $p = 4 \times 10^{-16}$; right amygdala: $p = 0.0006$).

To study the moderating effect of neurite architecture on this relationship, BOLD activity and NODDI indices (ODI or NDI) for left or right amygdala were entered into the first step of the regression analysis (together with age and sex). Entering the interaction term between ODI and BOLD activity (step 2 of the regression) resulted in a significant increase in variance explained in faces task performance (left amygdala: $\Delta R^2 = 0.01$, $F_{1, 744} = 7.37$, p (FDR-corrected) = 0.014; right amygdala: $\Delta R^2 = 0.02$, $F_{1, 744} = 11.61$, p (FDR-corrected) = 0.0028; Fig. 5, top row). Entering the interaction term between NDI and BOLD activity (step 2 of the regression) resulted in a significant increase in variance explained in faces task performance only in the right amygdala (left amygdala: $\Delta R^2 = 0.001$, $F_{1, 744} = 0.78$, p (FDR-corrected) = 0.76; right amygdala: $\Delta R^2 = 0.008$, $F_{1, 744} = 6.28$, p (FDR-corrected) = 0.050; Fig. 5, bottom row). Thus, neurite architecture was concluded to be a significant moderator of the relationship between BOLD activity and faces task performance. Given a non-normal distribution of the models' residuals, sensitivity analysis was conducted where p-values were calculated using permutation tests. The direction of results stayed the

same (FDR-corrected p-values; ODI left amygdala: $p = 4 \times 10^{-16}$; ODI right amygdala: $p = 8 \times 10^{-16}$; NDI left amygdala: $p = 0.24$; NDI right amygdala: $p = 0.0016$).

Faces task performance was significantly related to both left and right amygdala BOLD activity when ODI or NDI was one standard deviation (SD) above the mean (p (FDR-corrected) < 0.005) and when at the mean (p (FDR-corrected) < 0.05), but not when neurite architecture was one SD below the mean (p (FDR-corrected) > 0.05) (Fig. 5). See Supplementary Table 4 for detailed statistics.

4. Discussion

In this investigation of a large sample of young healthy adults, we found a relationship between gray matter neurite architecture and task-evoked BOLD activity. Lower ODI in DLPFC or ODI and NDI values in amygdala were related to higher BOLD activity, while common measures of brain macrostructure such as cortical thickness, surface area and subcortical volume did not explain any additional variance in BOLD activity. Our findings support the possibility that neurite architecture, i.e. gray matter microstructure, accounts for some variability in functional

brain activity. Additionally, a moderating effect of neurite architecture on the relationship between emotion processing task-evoked BOLD response in amygdala and performance was observed. Our findings expand our current knowledge about the microstructural underpinnings of the individual capacity of cognition and related brain activation in healthy adult brains.

We found that lower ODI, but not NDI, in DLPFC was related to higher BOLD activity during the working memory task. ODI may represent the branching and complexity (i.e., arborization) of dendritic trees in gray matter, while NDI maps onto neurite density in gray matter (that may reflect density of dendrites and myelinated fibers or myelin content) (Deligianni et al., 2016; Fukutomi et al., 2018; Grussu et al., 2017; Mah et al., 2017; Zhang et al., 2012). Recent evidence examining a smaller portion of the HCP sample reported distinct patterns of neurite architectural distribution across the cortex (Fukutomi et al., 2018). While NDI corresponded well with the distribution of myelin (myeloarchitecture) (Braak, 1980; Nieuwenhuys, 2013), ODI was interpreted as reflecting regional variations in the cortical cytoarchitecture (Von Economo, 2009; von Economo and Koskinas, 1925), showing high values in granular cortical areas (early sensory areas such as somatosensory, visual, and auditory cortices) and low in the agranular cortical areas (e.g., primary motor cortex, anterior insula, anterior cingulate). Importantly, regions associated with higher-order cognitive functions, including frontal and temporal cortices, had lower ODI values. Neurite architecture (ODI and to a lesser extent NDI) was also negatively associated with cortical thickness, especially lateral/medial aspects of the frontal cortex (including DLPFC) showing low ODI and relatively thick cortex (Fukutomi et al., 2018).

Our significant association with the BOLD response via cortical microstructure contrasts with our reported lack of association of BOLD with cortical macrostructure (e.g., cortical thickness), which has been noted in previous studies (Evangelista et al., 2021; Owens et al., 2018; Zacharopoulos et al., 2020). Cortical thickness and surface area did not provide any explanatory variance over and above that of ODI on the BOLD fMRI signal in DLPFC during the working memory task. Recent evidence initially linked higher intelligence directly to higher cortical volume and lower cortical ODI (and to a lesser extent to NDI) (Genç et al., 2018). One may speculate that while the efficient organization of the neurites/dendrites in DLPFC is crucial for efficient signal transmission (i.e., higher working memory-evoked BOLD activity) in the present study, the role of neurite density may be less important, supported by our recent study showing a tendency towards a negative relationship between ODI (but not NDI) and functional connectivity in the frontotemporal network (with key involvement in working memory performance) (Nazeri et al., 2015). It is possible that higher-performing participants benefit from more organized (i.e., less ramified) dendritic trees, since restricting synaptic connections to an efficient minimum facilitates the differentiation of signals from noise while saving network and energy resources (Genç et al., 2018), leading to better task-related brain activation ability and performance.

In the amygdala, we found a negative association of NDI with task-related BOLD activity and also of ODI with task-related BOLD activity. Both NDI and ODI explained a comparable amount of variance on emotion processing-evoked BOLD activity, unlike the DLPFC where only ODI explained variance. The specificity of ODI to BOLD activity in the DLPFC vs. the joint contribution of ODI and NDI to BOLD activity in the amygdala may have been driven by the fundamental differences of both regions with regard to evolution, function and structural organization. The DLPFC is a highly-organized, hierarchical structure (six distinct layers with strong interconnectivity (Amunts and Zilles, 2012); specific fiber orientation throughout the layers; and cell bodies arranged into (mini)columns (Buxhoeveden et al., 2000; Schlaug et al., 1995), enabling the high interconnectivity of cortical regions and strong connectivity with subcortical regions for efficient information transfer. The highly-evolved ability to modulate its connectivity distinguishes the DLPFC further from more primitive sensory cortex and subcortical structures (e.g., amygdala) (Arnsten and Jin, 2014). The amygdala (or "amyloid complex") is also characterized by stronger heterogeneity (composed of over 20 interconnected nuclei with distinct architecture, function and afferents/efferents (Swanson and Petrovich, 1998)) and simpler neuronal layering compared to DLPFC. The amygdala is highly connected to cortical and subcortical structures (Fossati, 2012), illustrated by extensive efferent and afferent fiber bundles enervating/leaving the major nuclei (Kedo et al., 2018). In a more complex, layered structure such as the DLPFC optimal organization of neurites interconnecting the different layers and columns (estimated by ODI) might be more important for brain function related to higher-order cognition. Whereas in amygdala, both the organization and the number/density of neurites (estimated via NDI) might be similarly important given the simpler, more time-dependent needs of emotion processing in the amygdala.

Finally, although we reported strong relationships between BOLD activity during working memory and emotion processing with task performance, mirroring former studies (e.g., Derntl et al., 2009; Habel et al., 2007; Manoach et al., 1997), we did not observe any moderating effect of neurite architecture on the relationship between working memory task-related BOLD activation in DLPFC and performance of the 2-back task. In contrast, gray matter neurite architecture in the amygdala moderated the relationship between emotion processing task-related BOLD activation and faces task performance. As neurite orientation dispersion and density (NDI only in right amygdala) increased, the effect of the BOLD response (i.e., the slope of BOLD activity and faces task performance) also increased. We found one study which reported that difficulties in recognition of facial emotional expressions during horizontal slit-viewing were linked to alterations in both NDI and ODI in clusters including the ventral occipital complex region, superior temporal/parietal association areas, and forceps major of the corpus callosum in patients with autism spectrum disorder (Yasuno et al., 2020). Overall, our results are novel and warrant replication (see "Limitations and future directions" section for potential further explanation).

It should be acknowledged that our effects of relationships between neurite architecture, brain function and cognition are fairly small (e.g., variance of 1–2% for BOLD activation vs NODDI indices regressions with correlation coefficients of $R = -0.13$ maximum). Recent brain-wide association studies of large datasets substantiate the evidence that fairly small effect sizes in associations between brain features (structure or function) and phenotypes (cognition or psychopathology) are normal and highly consistent across large neuroimaging study samples such as HCP, ABCD and UK-Biobank (median effect sizes between 0.02 and 0.03; range of $R = -0.15$ to 0.15, similar to the current study). On the other hand, studies with small sample size may show inflated effect sizes with fairly limited reproducibility (Marek et al., 2022). Additionally, a recent large study on the relationship between working memory-evoked BOLD activation and corresponding gray matter volume in the HCP sample ($n > 1000$) reported comparable small effects of significant brain-wide correlations (R ranging from a maximum of -0.111 to 0.151) (Owens et al., 2018). One explanation for the smaller variance shown between NODDI indices and BOLD response in our study and similar small effects on relationships between brain features and phenotypes shown by others (Marek et al., 2022; Owens et al., 2018) may relate to inter-subject variability in both brain activation patterns (Gordon et al., 2017; Hawco et al., 2021; Miller et al., 2012; Van Horn et al., 2008) as well as brain structure (Forde et al., 2020; Zilles and Amunts, 2013). Our results further suggest that the relationship between neurite architecture and task-related BOLD activity is complex and that other factors, apart from individual neurite architecture, play a role in driving individual cognitive task-evoked BOLD response. The findings of cross-sectional brain-behavior correlations being often small and unreliable without large samples urges "[…] human neuroscience towards study designs that either maximize sample sizes to detect small effects or maximize effect sizes using focused investigations" (Gratton et al., 2022).

Our present findings provide evidence that cognition-related BOLD activity is (at least partially) driven by the underlying local neurite or-

ganization and density with direct impact on cognition. In vivo gray matter microstructure represents a new target of investigation providing strong potential for translation into the clinic. In various psychiatric disorders, e.g. schizophrenia and autism spectrum disorder, postmortem-derived alterations in dendritic arborization and synaptic density (Berdenis van Berlekom et al., 2019; Martínez-Cerdeño, 2017) have been suggested to drive symptoms and alterations in brain function (Copf, 2016; Selemon and Zecevic, 2015), which could be recently confirmed by using novel in vivo gray matter microstructural imaging (Carper et al., 2016; D'Souza et al., 2021; Matsuoka et al., 2020; Nazeri et al., 2017; Onwordi et al., 2020; Parvathaneni et al., 2017). As data required for NODDI fitting (or other biophysically plausible models) can now be acquired in a clinically feasible time frame and setting, this tool opens up new possibilities for clinicians to more rapidly detect disease signatures and allows earlier intervention in the course of the disease. Given that neurites and gray matter microstructure have the capacity to rapidly remodel, these novel dMRI-based methods also represent an opportunity to non-invasively monitor neuroplastic changes post-therapy within much shorter time scales.

4.1. Limitations and future directions

A priori, we decided for an ROI-based rather than a whole brain-based analysis given that both tasks used have strong spatial specificity in activity patterns in core regions which are related to cognitive processing and task performance. It is well established that the DLPFC has a key function in working memory and shows pronounced activation upon working memory challenge (Barbey et al., 2013; Ragland et al., 2002). Similarly, the amygdala is a key player in emotional regulation and cognition with a clear activation pattern upon emotional challenge (Plichta et al., 2012; Sabatinelli et al., 2011; Vuilleumier et al., 2001). However, choosing a larger ROI instead of doing a vertex-/voxel-wise analysis may have reduced our effect of the relationship between neurite architecture and functional brain activity given that the peak effect/activation may have been within a small accumulation of vertices/voxels rather than the whole chosen ROIs.

It is important to acknowledge that the present sample consists exclusively of healthy, young adult individuals with generally good cognitive function. Given the changes in individual cytoarchitecture across the life span (Nazeri et al., 2015), a sample spanning a larger age range and including a geriatric population as well as individuals with lower cognitive function might allow for a more complete understanding of the relationship between functional brain activity and gray matter microstructure, particularly in the context of biological challenges and the implications for functional activity in the presence of microstructural deficits.

The moderating effect of gray matter neurite architecture on the relationship between emotion processing task-related BOLD activation and faces task performance in the amygdala may have been driven by the stronger variance in BOLD activity and task performance in participants with higher ODI and NDI values, and the limited variation in the participants with the highest performance may have produced a ceiling effect (Barch et al., 2013; West et al., 2021). In future studies this moderation should be reassessed using a more demanding emotion processing task to produce a higher variability and reduce a ceiling effect in performance to enable a better identification of the underlying neurite architecture-BOLD activation relationship. One could speculate that task performance may more directly (negatively) relate to neurite architecture in those studies.

5. Conclusion

We examined the neurophysiological role of NODDI indices (i.e., in vivo neurite architecture) in relation to cognition-evoked BOLD brain activity. We provided direct evidence linking ODI/NDI and BOLD activity in two separate tasks, with some differences between DLPFC (ODI

only) and amygdala (ODI and NDI). We conclude that neurite architecture may account for some variability in functional activity. The moderate variance between neurite architecture and task-related BOLD activity suggests that their relationship is complex and that other factors, apart from individual neurite architecture, may play a role in driving individual cognitive-task evoked BOLD response. In sum, NODDI model indices may play a unique role as structural correlates of fMRI signal underpinnings, particularly given a lack of association with cortical macrostructure.

Credit authorship contribution statement

Christin Schifani: Conceptualization, Methodology, Software, Formal analysis, Writing – original draft, Visualization. **Colin Hawco:** Conceptualization, Methodology, Writing – review & editing. **Arash Nazeri:** Methodology, Writing – review & editing. **Aristotle N. Voineskos:** Conceptualization, Resources, Writing – review & editing, Supervision, Funding acquisition.

Data and code availability statement

Data were provided by the Human Connectome Project, WU-Minn Consortium, downloaded from ConnectomeDB as part of the S900 release (http://db.humanconnectome.org). Data were accessed with permission of HCP.

Code is made available via github (https://github.com/cschifani/HCP_NODDIvsfMRI).

Supplementary materials

Supplementary material associated with this article can be found in the online version at doi:10.1016/j.neuroimage.2022.119575.

References

Ameis, S.H., Fan, J., Rockel, C., Voineskos, A.N., Lobaugh, N.J., Soorya, L., Wang, A.T., Hollander, E., Anagnostou, E., 2011. Impaired structural connectivity of socio-emotional circuits in autism spectrum disorders: a diffusion tensor imaging study. PLoS ONE 6 (11), e28044. doi:10.1371/journal.pone.0028044.

Amunts, K., Zilles, K., 2012. Architecture and organizational principles of Broca's region. Trends Cogn. Sci. 16 (8), 418–426. doi:10.1016/j.tics.2012.06.005.

Arnsten, A.F.T., Jin, L.E., 2014. Molecular influences on working memory circuits in dorsolateral prefrontal cortex. Prog. Mol. Biol. Transl. Sci. 122, 211–231. doi:10.1016/B978-0-12-420170-5.00008-8.

Barbey, A.K., Koenigs, M., Grafman, J., 2013. Dorsolateral prefrontal contributions to human memory. Cortex 49 (5), 1195–1205. doi:10.1016/j.cortex.2012.05.022.

Barch, D.M., Burgess, G.C., Harms, M.P., Petersen, S.E., Schlaggar, B.L., Corbetta, M., Glasser, M.F., Curtiss, S., Dixit, S., Feldt, C., Nolan, D., Bryant, E., Hartley, T., Footer, O., Bjork, J.M., Poldrack, R., Smith, S., Johansen-Berg, H., Snyder, A.Z., Van Essen, D.C.WU-Minn HCP Consortium, 2013. Function in the human connectome: task-fMRI and individual differences in behavior. Neuroimage 80, 169–189. doi:10.1016/j.neuroimage.2013.05.033.

Barr, M.S., Farzan, F., Rajji, T.K., Voineskos, A.N., Blumberger, D.M., Arenovich, T., Fitzgerald, P.B., Daskalakis, Z.J., 2013. Can repetitive magnetic stimulation improve cognition in schizophrenia? Pilot data from a randomized controlled trial. Biol. Psychiatry 73 (6), 510–517. doi:10.1016/j.biopsych.2012.08.020.

Berdenis van Berlekom, A., Muflihah, C.H., Snijders, G.J.L.J., MacGillavry, H.D., Middeldorp, J., Hol, E.M., Kahn, R.S., de Witte, L.D., 2019. Synapse pathology in schizophrenia: a Meta-analysis of postsynaptic elements in postmortem brain studies. Schizophr. Bull. 46 (2), 374–386. doi:10.1093/schbul/sbz060.

Braak, H., 1980. Architectonics of the human telencephalic cortex. Studies of brain function. Springer Berlin, Heidelberg doi:10.1007/978-3-642-81522-5.

Buxhoeveden, D.P., Switala, A.E., Roy, E., Casanova, M.F., 2000. Quantitative analysis of cell columns in the cerebral cortex. J. Neurosci. Methods 97 (1), 7–17. doi:10.1016/s0165-0270(99)00192-2.

Carper, R.A., Treiber, J.M., White, N.S., Kohli, J.S., Müller, R.-A., 2016. Restriction spectrum imaging as a potential measure of cortical neurite density in autism. Front. Neurosci. 10, 610. doi:10.3389/fnins.2016.00610.

Copf, T., 2016. Impairments in dendrite morphogenesis as etiology for neurodevelopmental disorders and implications for therapeutic treatments. Neurosci. Biobehav. Rev. 68, 946–978. doi:10.1016/j.neubiorev.2016.04.008.

Deligianni, F., Carmichael, D.W., Zhang, G.H., Clark, C.A., Clayden, J.D., 2016. NODDI and tensor-based microstructural indices as predictors of functional connectivity. PLoS ONE 11 (4), e0153404. doi:10.1371/journal.pone.0153404.

Derntl, B., Habel, U., Windischberger, C., Robinson, S., Kryspin-Exner, I., Gur, R.C., Moser, E., 2009. General and specific responsiveness of the amygdala during explicit emotion recognition in females and males. BMC Neurosci 10 (1), 91. doi:10.1186/1471-2202-10-91.

Dickie, E.W., Anticevic, A., Smith, D.E., Coalson, T.S., Manogaran, M., Calarco, N., Viviano, J.D., Glasser, M.F., Van Essen, D.C., Voineskos, A.N., 2019. Ciftify: a framework for surface-based analysis of legacy MR acquisitions. Neuroimage 197, 818–826. doi:10.1016/j.neuroimage.2019.04.078.

Drew, P.J., 2019. Vascular and neural basis of the BOLD signal. Curr. Opin. Neurobiol. 58, 61–69. doi:10.1016/j.conb.2019.06.004.

D'Souza, D.C., Radhakrishnan, R., Naganawa, M., Ganesh, S., Nabulsi, N., Najafzadeh, S., Ropchan, J., Ranganathan, M., Cortes-Briones, J., Huang, Y., Carson, R.E., Skosnik, P., 2021. Preliminary in vivo evidence of lower hippocampal synaptic density in cannabis use disorder. Mol. Psychiatry 26 (7), 3192–3200. doi:10.1038/s41380-020-00891-4.

Ehrlich, S., Brauns, S., Yendiki, A., Ho, B.-C., Calhoun, V., Schulz, S.C., Gollub, R.L., Sponheim, S.R., 2012. Associations of cortical thickness and cognition in patients with schizophrenia and healthy controls. Schizophr. Bull. 38 (5), 1050–1062. doi:10.1093/schbul/sbr018.

Ekstrom, A., 2010. How and when the fMRI BOLD signal relates to underlying neural activity: the danger in dissociation. Brain Res. Rev. 62 (2), 233–244. doi:10.1016/j.brainresrev.2009.12.004.

Evangelista, N.D., O'Shea, A., Kraft, J.N., Hausman, H.K., Boutzoukas, E.M., Nissim, N.R., Albizu, A., Hardcastle, C., Van Etten, E.J., Bharadwaj, P.K., Smith, S.G., Song, H., Hishaw, G.A., DeKosky, S., Wu, S., Porges, E., Alexander, G.E., Marsiske, M., Cohen, R., Woods, A.J., 2021. Independent contributions of dorsolateral prefrontal structure and function to working memory in healthy older adults. Cereb. Cortex 31 (3), 1732–1743. doi:10.1093/cercor/bhaa322.

Feinberg, D.A., Moeller, S., Smith, S.M., Auerbach, E., Ramanna, S., Gunther, M., Glasser, M.F., Miller, K.L., Ugurbil, K., Yacoub, E., 2010. Multiplexed echo planar imaging for sub-second whole brain FMRI and fast diffusion imaging. PLoS ONE 5 (12), e15710. doi:10.1371/journal.pone.0015710.

Forde, N.J., Jeyachandra, J., Joseph, M., Jacobs, G.R., Dickie, E., Satterthwaite, T.D., Shinohara, R.T., Ameis, S.H., Voineskos, A.N., 2020. Sex differences in variability of brain structure across the lifespan. Cereb. Cortex 30 (10), 5420–5430. doi:10.1093/cercor/bhaa123.

Fossati, P., 2012. Neural correlates of emotion processing: from emotional to social brain. Eur. Neuropsychopharmacol. 22 (Suppl 3), S487–S491. doi:10.1016/j.euroneuro.2012.07.008.

Fukutomi, H., Glasser, M.F., Zhang, H., Autio, J.A., Coalson, T.S., Okada, T., Togashi, K., Van Essen, D.C., Hayashi, T., 2018. Neurite imaging reveals microstructural variations in human cerebral cortical gray matter. Neuroimage 182, 488–499. doi:10.1016/j.neuroimage.2018.02.017.

Genç, E., Fraenz, C., Schlüter, C., Friedrich, P., Hossiep, R., Voelkle, M.C., Ling, J.M., Güntürkün, O., Jung, R.E., 2018. Diffusion markers of dendritic density and arborization in gray matter predict differences in intelligence. Nat. Commun. 9 (1), 1905. doi:10.1038/s41467-018-04268-8.

Glasser, M.F., Coalson, T.S., Robinson, E.C., Hacker, C.D., Harwell, J., Yacoub, E., Ugurbil, K., Andersson, J., Beckmann, C.F., Jenkinson, M., Smith, S.M., Van Essen, D.C., 2016a. A multi-modal parcellation of human cerebral cortex. Nature 536 (7615), 171–178. doi:10.1038/nature18933.

Glasser, M.F., Smith, S.M., Marcus, D.S., Andersson, J.L.R., Auerbach, E.J., Behrens, T.E.J., Coalson, T.S., Harms, M.P., Jenkinson, M., Moeller, S., Robinson, E.C., Sotiropoulos, S.N., Xu, J., Yacoub, E., Ugurbil, K., Van Essen, D.C., 2016b. The Human

Connectome Project's neuroimaging approach. Nat. Neurosci. 19 (9), 1175–1187. doi:10.1038/nn.4361.

Glasser, M.F., Sotiropoulos, S.N., Wilson, J.A., Coalson, T.S., Fischl, B., Andersson, J.L., Xu, J., Jbabdi, S., Webster, M., Polimeni, J.R., Van Essen, D.C., Jenkinson, M., 2013. The minimal preprocessing pipelines for the Human Connectome Project. Neuroimage 80, 105–124. doi:10.1016/j.neuroimage.2013.04.127.

Glasser, M.F., Van Essen, D.C., 2011. Mapping human cortical areas in vivo based on myelin content as revealed by T1- and T2-weighted MRI. J. Neurosci. 31 (32), 11597–11616. doi:10.1523/JNEUROSCI.2180-11.2011.

Gordon, E.M., Laumann, T.O., Adeyemo, B., Petersen, S.E., 2017. Individual variability of the system-level organization of the human brain. Cereb. Cortex 27 (1), 386–399. doi:10.1093/cercor/bhv239.

Gratton, C., Nelson, S.M., Gordon, E.M., 2022. Brain-behavior correlations: two paths toward reliability. Neuron 110 (9), 1446–1449. doi:10.1016/j.neuron.2022.04.018.

Greve, D.N., Fischl, B., 2009. Accurate and robust brain image alignment using boundary-based registration. Neuroimage 48 (1), 63–72. doi:10.1016/j.neuroimage.2009.06.060.

Grussu, F., Schneider, T., Tur, C., Yates, R.L., Tachrount, M., Ianuş, A., Yiannakas, M.C., Newcombe, J., Zhang, H., Alexander, D.C., DeLuca, G.C., Gandini Wheeler-Kingshott, C.A.M., 2017. Neurite dispersion: a new marker of multiple sclerosis spinal cord pathology? Ann Clin Transl Neurol 4 (9), 663–679. doi:10.1002/acn3.445.

Habel, U., Windischberger, C., Derntl, B., Robinson, S., Kryspin-Exner, I., Gur, R.C., Moser, E., 2007. Amygdala activation and facial expressions: explicit emotion discrimination versus implicit emotion processing. Neuropsychologia 45 (10), 2369–2377. doi:10.1016/j.neuropsychologia.2007.01.023.

Hall, C.N., Howarth, C., Kurth-Nelson, Z., Mishra, A., 2016. Interpreting BOLD: towards a dialogue between cognitive and cellular neuroscience. Philos. Trans. R. Soc. Lond. B Biol. Sci. 371 (1705), 20150348. doi:10.1098/rstb.2015.0348.

Hariri, A.R., Tessitore, A., Mattay, V.S., Fera, F., Weinberger, D.R., 2002. The amygdala response to emotional stimuli: a comparison of faces and scenes. Neuroimage 17 (1), 317–323. doi:10.1006/nimg.2002.1179.

Harms, R.L., Fritz, F.J., Tobisch, A., Goebel, R., Roebroeck, A., 2017. Robust and fast nonlinear optimization of diffusion MRI microstructure models. Neuroimage 155, 82–96. doi:10.1016/j.neuroimage.2017.04.064.

Hawco, C., Dickie, E.W., Jacobs, G., Daskalakis, Z.J., Voineskos, A.N., 2021. Moving beyond the mean: subgroups and dimensions of brain activity and cognitive performance across domains. Neuroimage 231, 117823. doi:10.1016/j.neuroimage.2021.117823.

Hawco, C., Yoganathan, L., Voineskos, A.N., Lyon, R., Tan, T., Daskalakis, Z.J., Blumberger, D.M., Croarkin, P.E., Lai, M.-C., Szatmari, P., Ameis, S.H., 2020. Greater individual variability in functional brain activity during working memory performance in young people with autism and executive function impairment. NeuroImage: Clinical 27, 102260. doi:10.1016/j.nicl.2020.102260.

Jacobs, G.R., Voineskos, A.N., Hawco, C., Stefanik, L., Forde, N.J., Dickie, E.W., Lai, M.-C., Szatmari, P., Schachar, R., Crosbie, J., Arnold, P.D., Goldenberg, A., Erdman, L., Ameis, S.H., 2021. Integration of brain and behavior measures for identification of data-driven groups cutting across children with ASD, ADHD, or OCD. Neuropsychopharmacology 46 (3), 643–653. doi:10.1038/s41386-020-00902-6.

Jessell, T.M., Kandel, E.R., 1993. Synaptic transmission: a bidirectional and self-modifiable form of cell-cell communication. Cell 72, 1–30. doi:10.1016/S0092-8674(05)80025-X.

Karantonis, J.A., Carruthers, S.P., Rossell, S.L., Pantelis, C., Hughes, M., Wannan, C., Cropley, V., Van Rheenen, T.E., 2021. A systematic review of cognition-brain morphology relationships on the schizophrenia-bipolar disorder spectrum. Schizophr. Bull. 47 (6), 1557–1600. doi:10.1093/schbul/sbab054.

Kaup, A.R., Mirzakhanian, H., Jeste, D.V., Eyler, L.T., 2011. A review of the brain structure correlates of successful cognitive aging. J. Neuropsychiatry Clin. Neurosci. 23 (1), 6–15. doi:10.1176/appi.neuropsych.23.1.6.

Kedo, O., Zilles, K., Palomero-Gallagher, N., Schleicher, A., Mohlberg, H., Bludau, S., Amunts, K., 2018. Receptor-driven, multimodal mapping of the human amygdala. Brain Struct. Funct. 223 (4), 1637–1666. doi:10.1007/s00429-017-1577-x.

Khalil, M., Hollander, P., Raucher-Chéné, D., Lepage, M., Lavigne, K.M., 2022. Structural brain correlates of cognitive function in schizophrenia: a meta-analysis. Neurosci. Biobehav. Rev. 132, 37–49. doi:10.1016/j.neubiorev.2021.11.034.

Lefebvre, J.L., Sanes, J.R., Kay, J.N., 2015. Development of dendritic form and function. Annu. Rev. Cell Dev. Biol. 31, 741–777. doi:10.1146/annurev-cellbio-100913-013020.

López, J.F., Akil, H., Watson, S.J., 1999. Neural circuits mediating stress. Biol. Psychiatry 46 (11), 1461–1471. doi:10.1016/s0006-3223(99)00266-8.

Mah, A., Geeraert, B., Lebel, C., 2017. Detailing neuroanatomical development in late childhood and early adolescence using NODDI. PLoS ONE 12 (8), e0182340. doi:10.1371/journal.pone.0182340.

Manoach, D.S., Schlaug, G., Siewert, B., Darby, D.G., Bly, B.M., Benfield, A., Edelman, R.R., Warach, S., 1997. Prefrontal cortex fMRI signal changes are correlated with working memory load. Neuroreport 8 (2), 545–549. doi:10.1097/00001756-199701200-00033.

Marek, S., Tervo-Clemmens, B., Calabro, F.J., Montez, D.F., Kay, B.P., Hatoum, A.S., Donohue, M.R., Foran, W., Miller, R.L., Hendrickson, T.J., Malone, S.M., Kandala, S., Feczko, E., Miranda-Dominguez, O., Graham, A.M., Earl, E.A., Perrone, A.J., Cordova, M., Doyle, O., Moore, L.A., Conan, G.M., Uriarte, J., Snider, K., Lynch, B.J., Wilgenbusch, J.C., Pengo, T., Tam, A., Chen, J., Newbold, D.J., Zheng, A., Seider, N.A., Van, A.N., Metoki, A., Chauvin, R.J., Laumann, T.O., Greene, D.J., Petersen, S.E., Garavan, H., Thompson, W.K., Nichols, T.E., Thomas Yeo, B.T., Barch, D.M., Luna, B., Fair, D.A., Dosenbach, N.U.F., 2022. Reproducible brain-wide association studies require thousands of individuals. Nature 603 (7902), 654–660. doi:10.1038/s41586-022-04492-9.

Martínez-Cerdeño, V., 2017. Dendrite and spine modifications in autism and related neurodevelopmental disorders in patients and animal models. Dev. Neurobiol. 77 (4), 393–404. doi:10.1002/dneu.22417.

Matsuoka, K., Makinodan, M., Kitamura, S., Takahashi, M., Yoshikawa, H., Yasuno, F., Ishida, R., Kishimoto, N., Yasuda, Y., Hashimoto, R., Taoka, T., Miyasaka, T., Kichikawa, K., Kishimoto, T., 2020. Increased dendritic orientation dispersion in the left occipital gyrus is associated with atypical visual processing in adults with autism spectrum disorder. Cereb. Cortex 30 (11), 5617–5625. doi:10.1093/cercor/bhaa121.

Miller, M.B., Donovan, C.-L., Bennett, C.M., Aminoff, E.M., Mayer, R.E., 2012. Individual differences in cognitive style and strategy predict similarities in the patterns of brain activity between individuals. Neuroimage 59 (1), 83–93. doi:10.1016/j.neuroimage.2011.05.060.

Morris, L.S., Kundu, P., Dowell, N., Mechelmans, D.J., 2016. Fronto-striatal organization: defining functional and microstructural substrates of behavioural flexibility. Cortex 74, 118–133. doi:10.1016/j.cortex.2015.11.004.

Nazeri, A., Chakravarty, M.M., Rotenberg, D.J., Rajji, T.K., Rathi, Y., Michailovich, O.V., Voineskos, A.N., 2015. Functional consequences of neurite orientation dispersion and density in humans across the adult lifespan. J. Neurosci. 35 (4), 1753–1762. doi:10.1523/JNEUROSCI.3979-14.2015.

Nazeri, A., Mulsant, B.H., Rajji, T.K., Levesque, M.L., Pipitone, J., Stefanik, L., Shahab, S., Roostaei, T., Wheeler, A.L., Chavez, S., Voineskos, A.N., 2017. Gray matter neuritic microstructure deficits in schizophrenia and bipolar disorder. Biol. Psychiatry 82 (10), 726–736. doi:10.1016/j.biopsych.2016.12.005.

Nazeri, A., Schifani, C., Anderson, J.A.E., Ameis, S.H., Voineskos, A.N., 2020. In Vivo imaging of gray matter microstructure in major psychiatric disorders: opportunities for clinical translation. Biol. Psychiatry Cogn. Neurosci. Neuroimag. 5 (9), 855–864. doi:10.1016/j.bpsc.2020.03.003.

Nieuwenhuys, R., 2013. The myeloarchitectonic studies on the human cerebral cortex of the Vogt-Vogt school, and their significance for the interpretation of functional neuroimaging data. Brain Struct. Funct. 218 (2), 303–352. doi:10.1007/s00429-012-0460-z.

Oliver, L.D., Haltigan, J.D., Gold, J.M., Foussias, G., DeRosse, P., Buchanan, R.W., Malhotra, A.K., Voineskos, A.N., 2019. Lower- and higher-level social cognitive factors across individuals with schizophrenia spectrum disorders and healthy controls: relationship with Neurocognition and functional outcome. Schizophr Bull 45 (3), 629–638. doi:10.1093/schbul/sby114.

Oliver, L.D., Moxon-Emre, I., Lai, M.-C., Grennan, L., Voineskos, A.N., Ameis, S.H., 2021. Social cognitive performance in schizophrenia spectrum disorders compared with autism spectrum disorder: a systematic review, meta-analysis, and meta-regression. JAMA Psychiatry 78 (3), 281–292. doi:10.1001/jamapsychiatry.2020.3908.

Onwordi, E.C., Halff, E.F., Whitehurst, T., Mansur, A., Cotel, M.-C., Wells, L., Creeney, H., Bonsall, D., Rogdaki, M., Shatalina, E., Reis Marques, T., Rabiner, E.A., Gunn, R.N., Natesan, S., Vernon, A.C., Howes, O.D., 2020. Synaptic density marker SV2A is reduced in schizophrenia patients and unaffected by antipsychotics in rats. Nat. Commun. 11 (1), 1–11. doi:10.1038/s41467-019-14122-0, 246.

Owens, M.M., Duda, B., Sweet, L.H., MacKillop, J., 2018. Distinct functional and structural neural underpinnings of working memory. Neuroimage 174, 463–471. doi:10.1016/j.neuroimage.2018.03.022.

Parvathaneni, P., Rogers, B.P., Huo, Y., Schilling, K.G., Hainline, A.E., Anderson, A.W., Woodward, N.D., Landman, B.A., 2017. Gray Matter Surface based Spatial Statistics (GS-BSS) in diffusion microstructure. Med. Image Comput. Comput. Assist. Interv. 10433, 638–646. doi:10.1007/978-3-319-66182-7_73.

Pera-Guardiola, V., Contreras-Rodríguez, O., Batalla, I., Kosson, D., Menchón, J.M., Pifarré, J., Bosque, J., Cardoner, N., Soriano-Mas, C., 2016. Brain structural correlates of emotion recognition in psychopaths. PLoS ONE 11 (5), e0149807. doi:10.1371/journal.pone.0149807.

Plichta, M.M., Schwarz, A.J., Grimm, O., Morgen, K., Mier, D., Haddad, L., Gerdes, A.B.M., Sauer, C., Tost, H., Esslinger, C., Colman, P., Wilson, F., Kirsch, P., Meyer-Lindenberg, A., 2012. Test–retest reliability of evoked BOLD signals from a cognitive–emotive fMRI test battery. Neuroimage 60 (3), 1746–1758. doi:10.1016/j.neuroimage.2012.01.129.

Ragland, J.D., Turetsky, B.I., Gur, R.C., Gunning-Dixon, F., Turner, T., Schroeder, L., Chan, R., Gur, R.E., 2002. Working memory for complex figures: an fMRI comparison of letter and fractal n-back tasks. Neuropsychology 16 (3), 370–379. doi:10.1037/0894-4105.16.3.370.

Robinson, E.C., Jbabdi, S., Glasser, M.F., Andersson, J., Burgess, G.C., Harms, M.P., Smith, S.M., Van Essen, D.C., Jenkinson, M., 2014. MSM: a new flexible framework for multimodal surface matching. Neuroimage 100, 414–426. doi:10.1016/j.neuroimage.2014.05.069.

Sabatinelli, D., Fortune, E.E., Li, Q., Siddiqui, A., Krafft, C., Oliver, W.T., Beck, S., Jeffries, J., 2011. Emotional perception: meta-analyses of face and natural scene processing. Neuroimage 54 (3), 2524–2533. doi:10.1016/j.neuroimage.2010.10.011.

Salthouse, T.A., 2011. Neuroanatomical substrates of age-related cognitive decline. Psychol. Bull. 137 (5), 753–784. doi:10.1037/a0023262.

Schlaug, G., Schleicher, A., Zilles, K., 1995. Quantitative analysis of the columnar arrangement of neurons in the human cingulate cortex. J. Comp. Neurol. 351 (3), 441–452. doi:10.1002/cne.903510310.

Selemon, L.D., Zecevic, N., 2015. Schizophrenia: a tale of two critical periods for prefrontal cortical development. Transl. Psychiatry 5 (8), e623. doi:10.1038/tp.2015.115.

Sergerie, K., Chochol, C., Armony, J.L., 2008. The role of the amygdala in emotional processing: a quantitative meta-analysis of functional neuroimaging studies. Neurosci. Biobehav. Rev. 32 (4), 811–830. doi:10.1016/j.neubiorev.2007.12.002.

Sotiropoulos, S.N., Jbabdi, S., Xu, J., Andersson, J.L., Moeller, S., Auerbach, E.J., Glasser, M.F., Hernandez, M., Sapiro, G., Jenkinson, M., Feinberg, D.A., Yacoub, E., Lenglet, C., Van Essen, D.C., Ugurbil, K., Behrens, T.E.J.WU-Minn HCP Consortium, 2013. Advances in diffusion MRI acquisition and processing in the Human Connectome Project. Neuroimage 80, 125–143. doi:10.1016/j.neuroimage.2013.05.057.

Swanson, L.W., Petrovich, G.D., 1998. What is the amygdala? Trends Neurosci 21 (8), 323–331. doi:10.1016/S0166-2236(98)01265-X.

Teillac, A., Lefrance, S., Duchesnay, E., Poupon, F., Ripoll Fuster, M.A., Le Bihan, D., Mangin, J.-F., Poupon, C., 2017. Colocalization of functional activity and neurite density within cortical areas. In: Computational Diffusion MRI, Mathematics and Visualization. Springer International Publishing, pp. 175–186.

Tsuchida, A., Laurent, A., Crivello, F., Petit, L., Joliot, M., Pepe, A., Beguedou, N., Gueye, M.F., Verrecchia, V., Nozais, V., Zago, L., 2021. The MRi-Share database: brain imaging in a cross-sectional cohort of 1,870 university students. Brain Struct. Funct. 226 (7), 2057–2085. doi:10.1007/s00429-021-02334-4.

Van Essen, D.C., Smith, S.M., Barch, D.M., Behrens, T.E.J., Yacoub, E., Ugurbil, K.WU-Minn HCP Consortium, 2013. The WU-minn human connectome project: an overview. Neuroimage 80, 62–79. doi:10.1016/j.neuroimage.2013.05.041.

Van Essen, D.C., Ugurbil, K., Auerbach, E., Barch, D., Behrens, T.E.J., Bucholz, R., Chang, A., Chen, L., Corbetta, M., Curtiss, S.W., Della Penna, S., Feinberg, D., Glasser, M.F., Harel, N., Heath, A.C., Larson-Prior, L., Marcus, D., Michalareas, G., Moeller, S., Oostenveld, R., Petersen, S.E., Prior, F., Schlaggar, B.L., Smith, S.M., Snyder, A.Z., Xu, J., Yacoub, E.WU-Minn HCP Consortium, 2012. The human connectome project: a data acquisition perspective. Neuroimage 62 (4), 2222–2231. doi:10.1016/j.neuroimage.2012.02.018.

Van Horn, J.D., Grafton, S.T., Miller, M.B., 2008. Individual variability in brain activity: a nuisance or an opportunity? Brain Imaging Behav 2 (4), 327–334. doi:10.1007/s11682-008-9049-9.

Voineskos, A.N., Blumberger, D.M., Schifani, C., Hawco, C., Dickie, E.W., Rajji, T.K., Mulsant, B.H., Foussias, G., Wang, W., Daskalakis, Z.J., 2021. Effects of repetitive transcranial magnetic stimulation on working memory performance and brain structure in people with schizophrenia spectrum disorders: a double-blind, randomized, sham-controlled trial. Biol. Psychiatry 6 (4), 449–458. doi:10.1016/j.bpsc.2020.11.011.

Von Economo, C., 2009. Cellular Structure of the Human Cerebral Cortex. Translated and Edited Version of 'Zellaufbau Der Grosshirnrinde des Menschen'(von Economo, 1927). Karger Medical and Scientific Publishers, Basel Translated and edited by Triarhou L.C.

von Economo, C.F., Koskinas, G.N., 1925. Die Cytoarchitektonik der Hirnrinde des erwachsenen Menschen. J. Springer, Berlin.

Vuilleumier, P., Armony, J.L., Driver, J., Dolan, R.J., 2001. Effects of attention and emotion on face processing in the human brain: an event-related fMRI study. Neuron 30 (3), 829–841. doi:10.1016/S0896-6273(01)00328-2.

West, H.V., Burgess, G.C., Dust, J., Kandala, S., Barch, D.M., 2021. Amygdala activation in cognitive task fMRI varies with individual differences in cognitive traits. Cogn. Affect. Behav. Neurosci. 21 (1), 254–264. doi:10.3758/s13415-021-00863-3.

Yasuno, F., Makinodan, M., Takahashi, M., Matsuoka, K., Yoshikawa, H., Kitamura, S., Ishida, R., Kishimoto, N., Miyasaka, T., Kichikawa, K., Kishimoto, T., 2020. Microstructural anomalies evaluated by neurite orientation dispersion and density imaging are related to deficits in facial emotional recognition via perceptual-binding difficulties in autism spectrum disorder. Autism Res. 13 (5), 729–740. doi:10.1002/aur.2280.

Yuan, P., Raz, N., 2014. Prefrontal cortex and executive functions in healthy adults: a meta-analysis of structural neuroimaging studies. Neurosci. Biobehav. Rev. 42, 180–192. doi:10.1016/j.neubiorev.2014.02.005.

Zacharopoulos, G., Klingberg, T., Cohen Kadosh, R., 2020. Cortical surface area of the left frontal pole is associated with visuospatial working memory capacity. Neuropsychologia 143, 107486. doi:10.1016/j.neuropsychologia.2020.107486.

Zatorre, R.J., Fields, R.D., Johansen-Berg, H., 2012. Plasticity in gray and white: neuroimaging changes in brain structure during learning. Nat. Neurosci. 15 (4), 528–536. doi:10.1038/nn.3045.

Zhang, H., Schneider, T., Wheeler-Kingshott, C.A., Alexander, D.C., 2012. NODDI: practical in vivo neurite orientation dispersion and density imaging of the human brain. Neuroimage 61 (4), 1000–1016. doi:10.1016/j.neuroimage.2012.03.072.

Zhao, K., Yan, W.-J., Chen, Y.-H., Zuo, X.-N., Fu, X., 2013. Amygdala volume predicts inter-individual differences in fearful face recognition. PLoS ONE 8 (8), e74096. doi:10.1371/journal.pone.0074096.

Zilles, K., Amunts, K., 2013. Individual variability is not noise. Trends Cogn. Sci. 17 (4), 153–155. doi:10.1016/j.tics.2013.02.003.